Journal of Luminescence 150 (2014) 40–45

Contents lists available at ScienceDirect

Journal of Luminescence

journal homepage: www.elsevier.com/locate/jlumin

~2 μm Luminescence properties and nonradiative processes of Tm^{3+} in silicate glass

Xueqiang Liu [a,b], Ming Li [a,b], Xin Wang [a,b], Feifei Huang [a,b], Yaoyao Ma [a,b], Junjie Zhang [c], Lili Hu [a], Danping Chen [a,*]

[a] Key Laboratory of Materials for High Power Laser, Shanghai Institute of Optics and Fine Mechanics, Chinese Academy of Sciences, Shanghai 201800, PR China
[b] Graduate School of Chinese Academy of Science, Beijing 100039, PR China
[c] College of Materials Science and Engineering, China Jiliang University, Hangzhou 310018, PR China

ARTICLE INFO

Article history:
Received 22 October 2013
Received in revised form
18 December 2013
Accepted 10 January 2014
Available online 29 January 2014

Keywords:
Tm^{3+}
Silicate glass
Fluoride
Emission cross sections
Quantum efficiency

ABSTRACT

Two novel Tm^{3+}-doped silicate glasses (one with fluoride addition) with good thermal stability were prepared in this work. Luminescence properties of these two samples were compared. After the addition of fluoride, the luminescence intensity of 1.8 μm was much improved whereas that of 1.47 μm was reduced. The rates of nonradiative processes populating and depopulating $^3F_4$ were calculated quantitatively and a new method of calculating the quenching rate of hydroxyls was proposed. It was found that multiphonon relaxation rate of $^3F_4 \rightarrow {}^3H_6$ was really low and could be neglected in both samples. The addition of fluoride in glass could reduce the quenching rate of hydroxyls but raised the cross-relaxation ($^3H_6 + {}^3H_4 \rightarrow {}^3F_4 + {}^3F_4$) rate. Thus the quantum efficiency of 1.8 μm luminescence was improved after the introduction of fluoride.

1. Introduction

Over the past decade, much attention has been paid to eye-safe ~2 μm lasers due to their important applications, such as mid-infrared remote sensing, light detection and ranging, laser medical applications, and pumping parametric oscillators [1–4]. Infrared laser oscillation using Tm^{3+} as an active ion can be obtained in the 1.8–2.2 μm range with the $^3F_4 \rightarrow {}^3H_6$ transition when the $^3H_4$ state is excited by an 808 nm laser diode (LD). Thanks to the cross-relaxation ($^3H_6 + {}^3H_4 \rightarrow {}^3F_4 + {}^3F_4$) process between Tm^{3+} ions, the ideal quantum efficiency of Tm^{3+}:$^3F_4$ ion can be 2. Hence, till now, laser output has been realized in various glass matrices [5–8]. However, few researches have been focused on the detailed mechanism of 1.8 μm in Tm^{3+}-doped silicate glass.

Silicate glass is a promising material in realizing 2 μm lasers. Compared to silica glass, it has a higher solubility of rare earth ions and smaller maximum phonon energy due to its less defined structure [9]. In some cases, single-frequency laser operation for example, a much shorter fiber is required to achieve high gain ability [10]. Here silicate glass is a more appropriate material than silica. Though the larger multiphonon relaxation rate induced by higher phonon energy in silicate glass (~1000 cm^{-1}), compared with other multicomponent glass such as fluoride and heavy metal glass, lowers the quantum efficiency of ~2 μm luminescence, it turns out that the slope efficiency in the silicate fiber lasers can be much higher than that in other glass fibers [4,6–8].

Apart from multiphonon relaxation process, some other nonradiative processes also play important roles in the 1.8 μm luminescence, including cross-relaxation process CR($^3H_6 + {}^3H_4 \rightarrow {}^3F_4 + {}^3F_4$) and energy transfer to impurities such as hydroxyls and transition metals. By increasing the population of $^3F_4$, the cross relaxation process contributes to 1.8 μm luminescence. In contrast, impurities are strong quenching centers of 1.8 μm luminescence. The transition metals can be avoided by using high-purity raw materials. To eliminate hydroxyls in the glass, various methods have been devised, for example, bubbling dry oxygen, bubbling dry $O_2 + CCl_4$ mixture [11], addition of halide and so on. Although much work has been carried out to remove hydroxyls, few focused on the quantitative analysis of the quenching effect by hydroxyls in rare-earth ion doped glass. Zhang et al. proposed a method to calculate it by comparing the lifetime of rare earth ion in tetraphosphate glasses with different contents of hydroxyls, which is based on that quenching rate by hydroxyls is positively correlated to the product of concentrations of rare earth ions and hydroxyls [12]. Yan et al. discussed the quenching rate of Er^{3+} by hydroxyls in phosphate glasses by assuming that only part of hydroxyls are coupled to rare

---

* Corresponding author. Tel.: +86 21 59911975.
E-mail address: dpchen2008@aliyun.com (D. Chen).

0022-2313/$ - see front matter © 2014 Elsevier B.V. All rights reserved.
http://dx.doi.org/10.1016/j.jlumin.2014.01.030

earth ions [13]. All of these work start from the interaction mechanism between rare earth ions and hydroxyls and a number of assumptions are made, which reduce the accuracy of results.

In this work, by combining rate equations and luminescent spectra of two samples, a new method of calculating quenching rate by hydroxyls is devised. During the calculation, luminescent properties of these two glasses are compared. The excellent physical property together with good luminescent property indicates the high potential of SACBF for 2 μm fiber lasers.

2. Experimental

2.1. Material synthesis

The compositions of two kinds of silicate glasses $56SiO_2$–$5Al_2O_3$–$20CaO$–$19BaO$–$1Tm_2O_3(1Eu_2O_3)$ and $56SiO_2$–$5Al_2O_3$–$20CaO$–$14BaO$–$5BaF_2$–$1Tm_2O_3(1Eu_2O_3)$ are named SACB and SACBF, respectively. Eu_2O_3 doped samples are used for phonon sideband spectra analysis. Analytical grades of SiO_2, $Al(OH)_3$, $CaCO_3$, $BaCO_3$ and BaF_2 are used as raw materials. First of all, 40-g batches of the samples are weighed and mixed. The samples are melted in a platinum crucible at 1450 °C for 1 h. Then the melts are poured into a preheated mold and annealed for 4 h near the glass transition temperature before they are cooled to room temperature. Finally, the annealed samples are fabricated and polished to the size of $10 \times 10 \times 1$ mm^3 for the optical and spectroscopic measurements, whereas others are cut and polished for refractive index.

2.2. Measurements

The refractive index is measured by the prism coupler method. The density is measured by the Archimedes method using distilled water as the immersion liquid. The characteristic temperatures (temperature of glass transition T_g) of powder samples crushed down from the samples are determined by a NetzschSTA449/C differential scanning calorimeter (DSC) at a heating rate of 10 K/min. In addition, the absorption spectra are recorded with a Perkin-Elmer Lambda 900 UV/VIS/NIR spectrophotometer in the range of 300–2100 nm. Furthermore, the excitation spectra of Eu^{3+} are detected upon emission at 614 nm and emission spectra of Tm^{3+} are measured upon excitation at 808 nm, both on the Triax 320 type spectrometer (Jobin-Yvon Co., France). For the lifetime measurements of the Tm^{3+}:$^3F_4$ state, the instrument applied is an FLSP 920 (Edinburgh instruments Ltd., UK). All the measurements are carried out at room temperature.

Table 1
Density ρ, molar volume V_M, concentration of Tm^{3+} N_0, refractive index n_R at 632.8 nm and ΔT in SACB and SACBF.

	ρ (g/cm^3)	V_M (cm^3)	N_0 (10^{20} cm^{-3})	n_R	ΔT ($T_x - T_g$)
SACB	3.46	25.41	4.5	1.61	∞
SACBF	3.59	24.79	4.8	1.604	274

3. Results and discussion

3.1. Physical properties and hydroxyl content of SACB and SACBF

Table 1 compares density ρ, molar volume V_M, refractive index n_R at 632.8 nm and ΔT in SACB and SACBF. The incorporation of F^- ions can create more network terminating (NT) sites, producing interstitial sites for large cations (e.g. Ba^{2+}) in the glass [14]. Thus substitution of barium oxide by barium fluoride raises the density but decreases the molar volume of glass. Compared to SACB, n_R of SACBF is smaller due to the smaller polarizability of fluoride than oxide [14]. The concentration of Tm^{3+} in SACB and SACBF is 4.5×10^{20} cm^{-3} and 4.8×10^{20} cm^{-3}, respectively. As is shown in Fig. 1(a) and (b), Tg in SACB is much larger than that in SACBF and there is no crystallization peak in SACB, indicating its good thermal stability [15]. After the addition of fluoride, though crystallization peak appears in the DSC curve, ΔT in SACBF is still large, indicating its strong ability against crystallization.

The presence of OH^- groups strongly affects IR fluorescence lifetimes of RE^{3+} ions in rare-earth doped systems [12]. It has been demonstrated that OH^- is one of the dominant quenching centers in Tm^{3+} doped glasses [9], especially for populations of $^3F_4$ and $^3H_4$ levels, because only a few hydroxyls (2700–3700 cm^{-1}) are required for nonradiative de-excitation through multiphonon relaxation. In this work, bubbling with oxygen is used to eliminate the OH^- in the glass. The OH^- content in the glass can be expressed by the absorption coefficient of the OH^- vibration band at ~3.3 μm, which is given by [9]

$$\alpha_{OH^-} = \frac{\ln(T_0/T)}{l} \qquad (1)$$

where l is the thickness of a sample whereas T_0 and T are the transmitted and incident intensities, respectively.

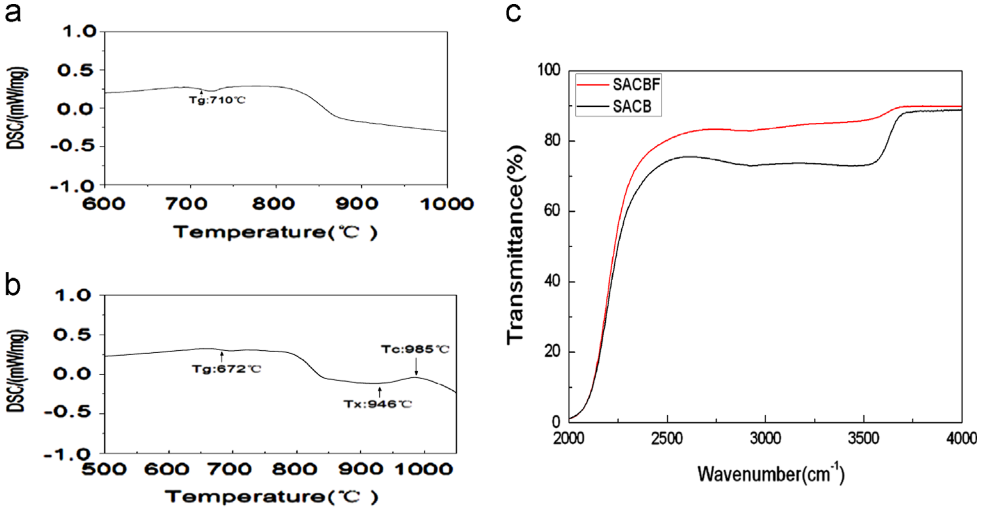

Fig. 1. DSC curve of SACB (a) and SACBF (b), near-infrared transmittance spectra (c) of SACBF and SACB.